J. Micromech. Microeng. **19** (2009) 125029 (8pp) doi:10.1088/0960-1317/19/12/125029

Characterization of heavily doped polysilicon films for CMOS-MEMS thermoelectric power generators

Jin Xie[1], Chengkuo Lee[1,2], Ming-Fang Wang[1], Youhe Liu[1] and Hanhua Feng[1]

[1] Institute of Microelectronics, A*STAR (Agency for Science, Technology and Research), 11 Science Park Road, Singapore Science Park II, Singapore 117685
[2] Department of Electrical and Computer Engineering, National University of Singapore, 4 Engineering Drive 3, Singapore 117576

E-mail: xiej@ime.a-star.edu.sg and elelc@nus.edu.sg

Received 4 September 2009, in final form 15 October 2009
Published 16 November 2009
Online at stacks.iop.org/JMM/19/125029

Abstract
This paper presents the material characterization of boron- and phosphorus-doped LPCVD polysilicon films for the application of thermoelectric power generators. Electrical resistivity, Seebeck coefficient and thermal conductivity of polysilicon films doped with doses from 4×10^{15} to 10×10^{15} at cm^{-2} have been measured at room temperature. Specific contact resistance between polysilicon and aluminum is studied and nickel silicidation is formed to reduce the contact resistance. The overall thermoelectric properties, as characterized by the figure of merit, are reported for polysilicon doped with different doping concentrations. For the most heavily doping dose of 10×10^{15} at cm^{-2}, figure of merit for p- and n-type polysilicon is found as 0.012 and 0.014, respectively. Based on the characterization results, a CMOS compatible thermoelectric power generator composed of boron- and phosphorus-doped polysilicon thermopiles is fabricated. When 5 K temperature difference is maintained across two sides of a device of size of 1 cm^2, the output power is 1.3 μW under a matched electrical resistance load.

1. Introduction

As a kind of energy harvesting device, thermoelectric power generators (TPGs) have been investigated to generate electricity from temperature difference due to the thermoelectric Seebeck effect. One of the scenarios is harvesting body heat as an alternative power source to enable applications such as self-sustained wearable electronics, body area sensor networks, etc [1, 2]. A thermocouple is made of two different thermoelectric bars joined at one end. TPGs are composed of a large number of thermocouples which are electrically connected in series. Thermoelectric materials are characterized by a dimensionless figure-of-merit parameter (ZT):

$$ZT = \frac{\alpha^2}{\rho\lambda}T, \quad (1)$$

where α is the Seebeck coefficient, ρ is the electrical resistivity, λ is the thermal conductivity and T is the temperature.

Currently, most commercial TPGs [3] use Bi_2Te_3 as thermoelectric material due to its large thermoelectric figure of merit. However, Bi_2Te_3 and its alloy are not CMOS compatible materials, which means Bi_2Te_3 materials based approaches cannot provide a TPG to be monolithically integrated on microelectronics and fabricated in normal CMOS manufacturing lines. Integration of TPGs with microelectronics to form a self-sustained system-on-chip device is a goal receiving a lot of research attention. Having TPGs fabricated by the standard CMOS process is necessary to achieve such a goal.

On the other hand, high thermoelectric performance has been found in single crystal silicon nanowires recently [4, 5], however, great challenges exist to fabricate TPGs with silicon nanowires, such as electrical connection of a large number

of p- and n-type silicon nanowires in series. Thus, the research on silicon nanowires for thermoelectric applications is still at its infant stage. Most of the publications in this field are related to material characterization. Doped polysilicon has attracted wide research interest for applications of TPGs due to its CMOS compatibility and widely available processing capability. Various TPGs based on p- and n-type doped polysilicon have been proposed and developed, but most of them have poor output power due to the low figure of merit of polysilicon [6–8]. To improve the performance of the TPGs, thermoelectric properties of doped polysilicon need to be characterized and optimized. In the late 1990s, research efforts were made to investigate the material properties of polysilicon and other CMOS materials in view of promising applications of various microelectromechanical systems (MEMS) based CMOS sensors [9], e.g. thermopiles, Pirani sensors, microbolometers, etc. For example, Paul *et al* gave the first overview of measured thermophysical properties of gate polysilicon and capacitor thin films [10], and von Arx *et al* fabricated test structures to measure the Seebeck coefficient [11] and thermal conductivity [12] of polysilicon of commercial CMOS IC processes in a wide temperature range from 120 to 400 K. All these authors focused on the measurement of polysilicon film produced by standard CMOS processes, and did not discuss the effect of doping concentration. Boutchich *et al* [13] characterized Seebeck coefficient of boron and phosphorus heavily doped LPCVD polysilicon films with different doses in the temperature range of 293–373 K. McConnell *et al* [14] provided a thermal modeling for polysilicon and verified the modeling by measuring thermal conductivity at different processing conditions and dopant concentrations. Later on, Strasser demonstrated micromachined TPGs using thermocouples made of polysilicon and characterized the materials at different doping concentrations in 2004, but figure of merit was not discussed in this paper in order to optimize the material properties for TPGs [6]. Additionally, PolySiGe as another CMOS compatible material has also been characterized for its thermoelectric properties [15, 16].

This paper presents the characterization of material properties of boron- and phosphorus-doped polysilicon to optimize the performance of TPGs. The characterized properties include electrical resistivity, specific contact resistance, Seebeck coefficient and thermal conductivity. This paper first studies how these properties are affected by doping doses in a range from 4×10^{15} to 10×10^{15} at cm^{-2}. Special test structures are designed to characterize the above properties of polysilicon films at room temperature. Figure of merit of doped polysilicon for each doping dose is discussed and compared with the values from the literature. Based on the optimized thermoelectric material properties, a CMOS compatible TPG using p- and n-doped polysilcon thermopiles is fabricated, and the output power from the TPG is measured. Our approach shows optimized polysilicon TPG performance, which is better than reported data from the other groups.

Table 1. Implant energy for doping polysilicon layers.

	Implant energy (keV)	
Doping dose (at cm^{-2})	Boron doped	Phosphorus doped
4×10^{15}	70	100
6×10^{15}	70	130
8×10^{15}	80	160
10×10^{15}	80	180

2. Fabrication and characterization

To prepare polysilicon samples for testing, 700 nm thick polysilicon layers are grown at 580 °C in furnace by low-pressure chemical vapor deposition (LPCVD). The polysilicon layers are partially implanted by boron (p-type) and phosphorus (n-type) from 4×10^{15} to 10×10^{15} at cm^{-2} doses. The implant energy for each group doses is shown in table 1. Afterward, the doped polysilicon layers are annealed in furnace at 1000 °C for 30 min to activate dopants and obtain a uniform doping profile through the whole thickness and repair the defects in the crystalline structure.

2.1. Electrical resistivity and specific contact resistance

Low electrical resistivity of polysilicon and low specific contact resistance between polysilicon and metals is highly desired in a micromachined TPG composed of a large number of thermocouples. The electrical resistivity is determined by the van-der-Pauw structure, and the measured values at different doping doses at room temperature are shown in figures 1(*a*) and (*b*). It is found that the higher the doping dose, the lower is the electrical resistivity. The electrical contact resistance is derived via the Kelvin structure [17], as shown in figure 2(*a*). An effective way to reduce contact resistance is creating nickel silicidation layer between polysilicon and metal. The process of formation of nickel silicidaiton is described as follows: after deposition and pattern of polysilicon, metal (here Al/TaN) and oxide dielectric layer, 135 Å thick nickel is deposited by sputtering; and then the silicidation step is done by a thermal reaction using rapid thermal processing (RTP) at 480 °C for 30 s; finally, the unreacted nickel is etched using H_2SO_4:H_2O_2 = 4:1 solution at 90 °C for 5 min. Transmission electron microscopy (TEM) analyzes that the component of nickel silicidation is NiSi (as shown in figure 2(*b*)), which has lower resistivity than other forms of nickel silicidation do, such as Ni_2Si and $NiSi_2$ [18, 19]. Without nickel silicidation, the specific contact resistance is 360 Ω μm^2 for p-type and 477 Ω μm^2 for n-type polysilicon. However, with the formation of nickel silicidation between polysilicon and aluminum alloy, the specific contact resistance is only about one quarter of the values, i.e., 95 Ω μm^2 for p-type and 123 Ω μm^2 for n-type polysilicon.

2.2. Seebeck coefficient

Seebeck coefficient was measured by a planar test structure, as shown in figure 3. The polysilicon stripe sample being

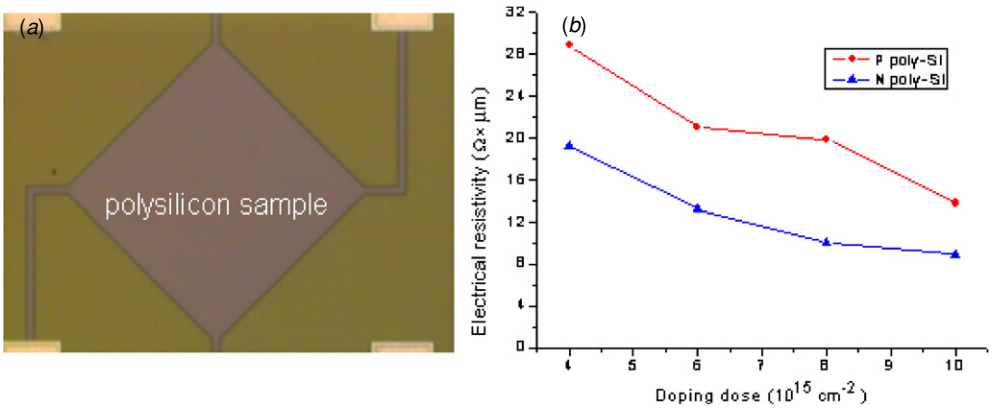

Figure 1. (*a*) Van de Pauw structure and (*b*) electrical resistivity of polysilicon at different doping doses.

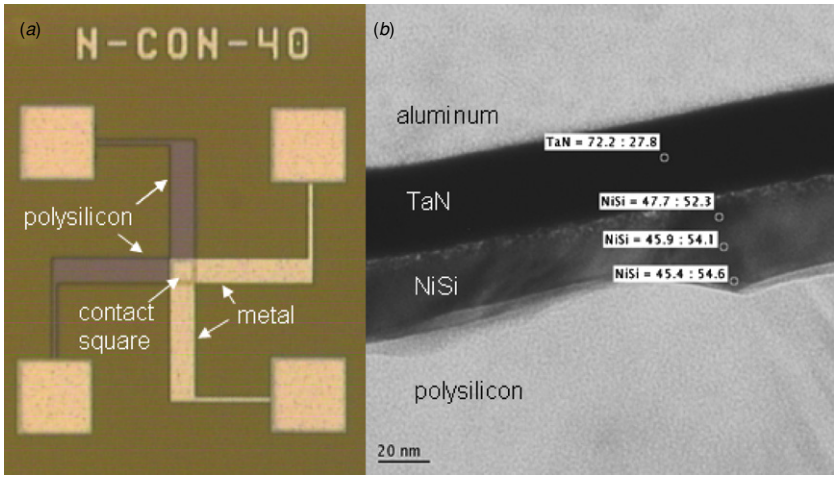

Figure 2. (*a*) Kelvin structure and (*b*) TEM of NiSi silicidation between polysilicon and Al/TaN.

characterized has a length of 670 μm and a width of 30 μm. It is contacted to aluminum at its two ends (pads 5 and 6). A 110 μm × 20 μm polysilicon heater (pads 11 and 12) is placed 20 μm away from the contact of the hot junction. Two 5 μm wide temperature monitors made of aluminum are placed over these two contacts. The temperature monitors are integrated in a four-point measurement configuration (pads 1, 2, 3, 4 and 7, 8, 9, 10) enabling accurate measurements of small resistance changes and, thus, small temperature variations. When applying current to the heating resistor, the temperature of the hot and cold contacts of the polysilicon sample was increased from T_0 to T_h and T_c, respectively. The Seebeck coefficient was expressed by

$$\alpha|_{\frac{T_h+T_c}{2}} = \frac{U}{T_h - T_c} = \frac{U}{\Delta T}, \tag{2}$$

where U is thermovoltage between the two ends of polysilicon. The measurement consisted of determining the temperature increases ΔT of each thermistor under a dissipated heat power and simultaneously measuring the thermovoltage U. We determined ΔT using the temperature-dependent resistance $R(T)$ of the temperature monitors, via their temperature coefficient of resistance (TCR) $\beta(T)$ defined as

$$\beta(T) = R(T)^{-1} \frac{\mathrm{d}}{\mathrm{d}T} R(T). \tag{3}$$

For this purpose, $R(T)$ curves were measured independently for each temperature sensing resistor of each test structure to take into account possible variations in material properties. Resistance $R(T_i)$ was measured at each temperature T_i ($i = 1, 2, \ldots, 19$), under stabilized temperature conditions. From the resistance data, values of $\beta(T_i)$ ($i = 2, 3, \ldots, 18$), were calculated for each temperature sensing resistor of each test structure using finite difference, i.e.,

$$\beta(T_i) = R(T_i)^{-1} \frac{R(T_{i+1}) - R(T_{i-1})}{T_{i+1} - T_{i-1}}. \tag{4}$$

As an example of boron-doped polysilicon with dose of 10×10^{15} at cm^{-2}, figure 4 shows the temperature-dependent resistance of the aluminum resistors and its TCR. At $T =$ 300 K, the electrical resistance of the aluminum-based alloy resistor was 0.166 Ω and β was 3.8×10^{-3} K^{-1}. According to the dimension of the resistor, the electrical resistivity of the aluminum-based alloy was calculated as 3.15×10^{-8} Ω m at $T = 300$ K.

For the thermovoltage measurements, a heating current I_h was passed through the heating resistor. The resulting resistance change ΔR of the temperature monitors was

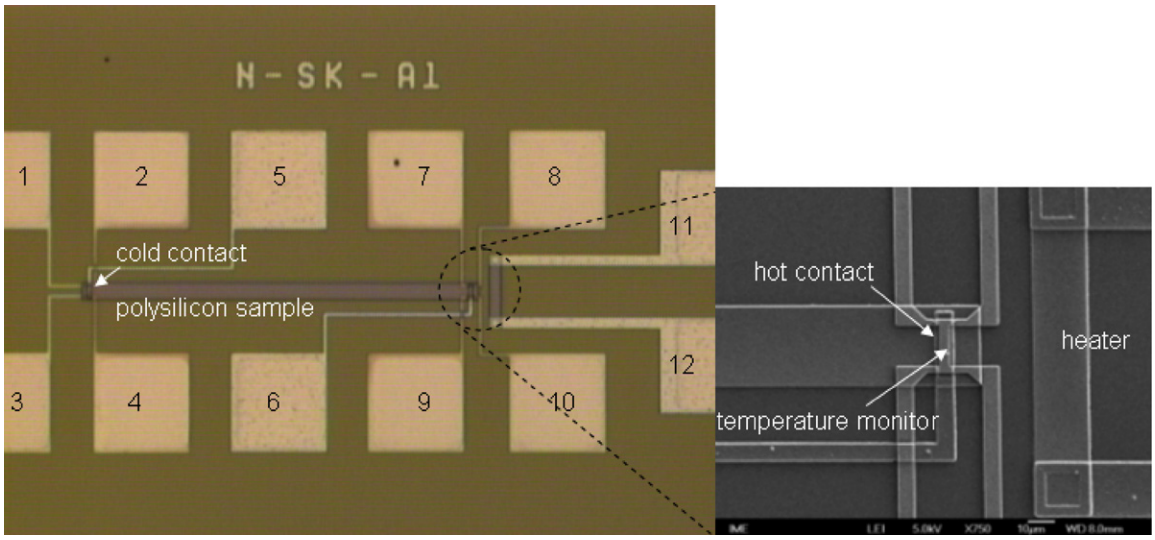

Figure 3. Test structure to determine the Seebeck coefficient.

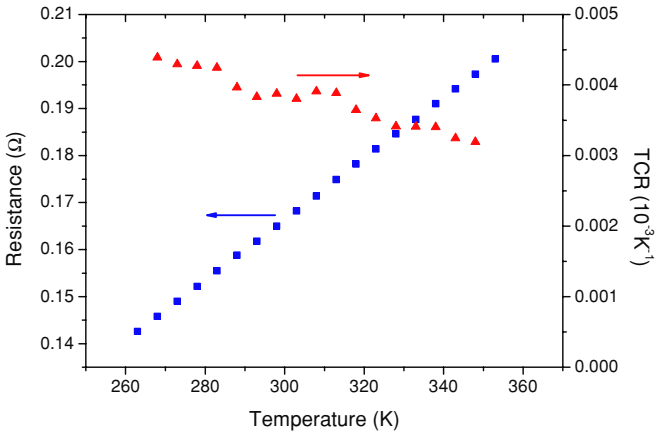

Figure 4. Temperature-dependent resistance and TCR of the aluminum temperature monitors.

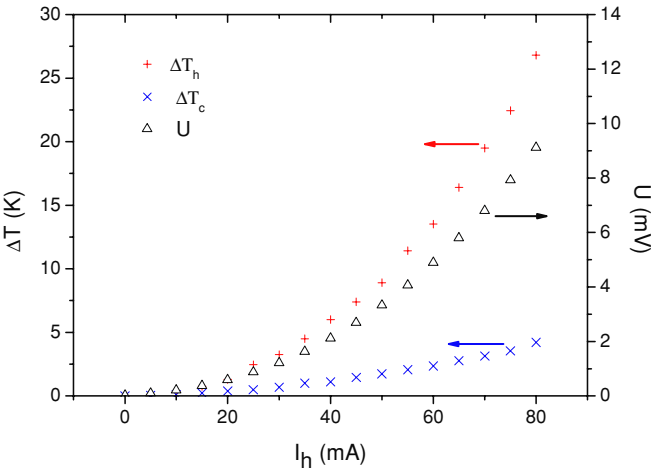

Figure 5. Thermovoltage as a function of heater current.

measured simultaneously. The temperature increases ΔT were obtained using

$$\Delta T = \frac{1}{\beta}\frac{\Delta R}{R}. \tag{5}$$

Simultaneously with the ΔR measurement we recorded the thermovoltage U. For the example of boron-doped polysilicon with 10×10^{15} at cm^{-2} doses, figure 5 shows the experimental data of the thermovoltage and temperature increases as a function of the heating current I_h at $T_0 = 300$ K. Based on the raw data, the Seebeck coefficient α of the polysilicon was calculated using equation (2). Figure 6 shows the measured Seebeck coefficient at room temperature for both doped p-type and n-type polysilicon with different doping doses.

2.3. Thermal conductivity

Thermal conductivity was determined by a cantilever composed of three layers: thermal oxide, LPCVD polysilicon and PECVD oxide, as shown in figure 7. A 100 μm wide and 270 μm long beam with four narrow arms is suspended over a cavity. Two contacts made of aluminum (pads 5 and 6) are used to measure the thermally generated voltage from the polysilicon sample. The hot contact is placed 23 μm away from the tip end of the cantilever, and the cold contact is on the substrate. Two resistors made of polysilion are integrated into the tip of the cantilever. The resistor (pads 1 and 2) close to the end of the beam is used as a heater, which has length of 92 μm, width of 6 μm and resistance of 2635 Ω at $T = 300$ K. The other resistor (pads 3 and 4) is used as temperature monitor, with total length of 280 μm and width of 1 μm. The temperature distribution over the top of the two resistors is homogenized with an integrated rectangular cover made of aluminum. This minimizes the temperature difference between the hot contact and temperature monitor. The cantilever was released by isotropic silicon etching with SF_6 gas. When a power P was dissipated in the heater, the temperature on the cantilever tip was increased by ΔT with respect to the substrate temperature. The heating power P and ΔT are related by $P = G \cdot \Delta T$, where G denotes the overall thermal conductance of the structure, including cantilever and

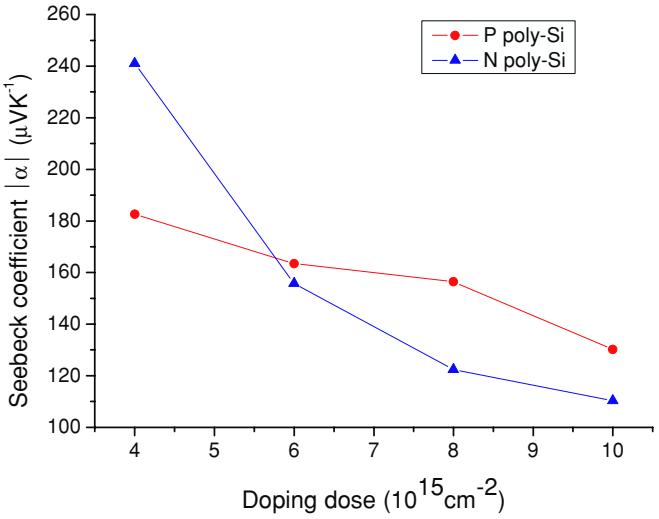

Figure 6. Seebeck coefficient of polysilicon at different doping doses.

connection arms. The heat flow between the heater and silicon support is essentially one dimensional. Heat loss by radiation and convection of the beam, and by conductance of connection arms was ignored because they contribute no more than 6% of the total thermal conductance [12]. Therefore, we got

$$G = \lambda_{\text{poly-Si}} \frac{t_{\text{poly-Si}} w}{l} + \bar{\lambda}_{\text{oxide}} \frac{t_{\text{oxide}} w}{l}, \tag{6}$$

where l and w are the length and width of the cantilever, $t_{\text{poly-Si}}$ and t_{oxide} are the thickness of polysilicon and oxide, respectively. The average thermal conductivity of thermal oxide and PECVD oxide $\bar{\lambda}_{\text{oxide}}$ is 1.1 W m^{-1} K^{-1} [12]. Heating current I_{h} passed through the heater and the heating power P was calculated as $P = I_{\text{h}}^2 R$, where R was the resistance of the heater. The temperature increase ΔT of cantilever was determined using the temperature-dependent resistance of the polysilicon temperature monitor via its TCR. As an example, figure 8 shows the temperature-dependent resistance and TCR of the polysilicon temperature monitor.

Finally, the overall thermal conductance for cantilever was calculated by $G = P/\Delta T$, and then thermal conductivity of polysilicon was obtained by equation (3). The measured thermal conductivity for doped polysilicon layer at 300 K with different doping doses is shown in figure 9. For a given dopant type, the sample with the higher dopant concentration has lower thermal conductivity values since larger number of impurities provide more scattering sites for the phonons [14]. At a given dopant concentration, layers doped with phosphorus have higher thermal conductivity values than boron-doped layers.

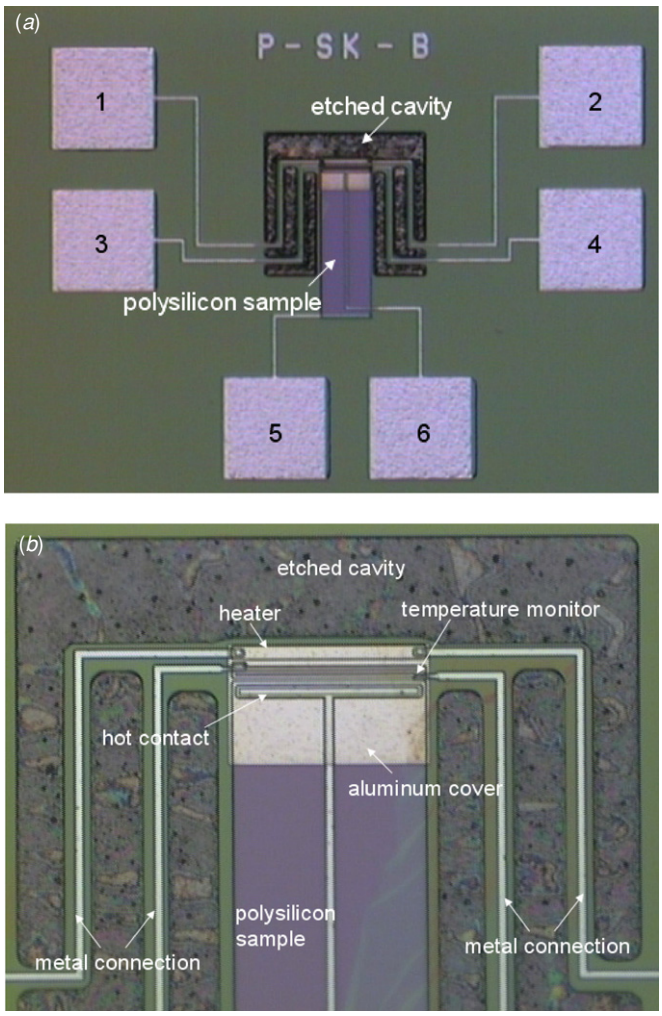

Figure 7. (*a*) Test structure to determine thermal conductivity and (*b*) a close-up view of the tip of cantilever.

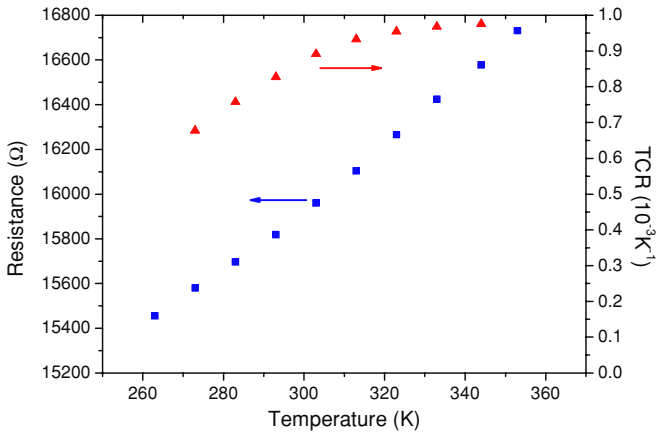

Figure 8. Temperature-dependent resistance and TCR of the polysilicon temperature monitor.

3. Discussion

From the measured result, it is found that for both p-type and n-type polysilicon, the higher the doping dose, the lower is the electrical resistivity, Seebeck coefficient and thermal conductivity. This can be explained by the fact that the dopant atoms increase charge carrier concentration and cause phonon scattering. According to the characterized electrical resistivity, Seebeck coefficient and thermal conductivity, the figure of merit for the investigated polysilicon films has been calculated for each doping dose, as shown in figure 10. It is seen that for

Table 2. Summarization of characterization of thermoelectric properties for polysilicon and polySiGe at $T = 300$ K.

Material		Electrical resistivity ($\Omega\ \mu$m)	Seebeck coefficient (μV K^{-1})	Thermal conductivity (W m^{-1} K^{-1})	Figure of merit	Reference
Polysilicon	p	22.1	103	31.2	0.005	[6]
	n	8.1	−57	31.5	0.004	
	p	13.7	130	28.4	0.012	This work (for dose of 10×10^{15} at cm^{-2})
	n	8.9	−110	29.7	0.014	
PolySiGe	p	28.9	131	4.7	0.037	[15]
	n	29.2	−179	5.1	0.061	
	p	11	35	∼3.5	0.01–0.02	[16]
	n	62	−190	∼3.5	0.04–0.05	

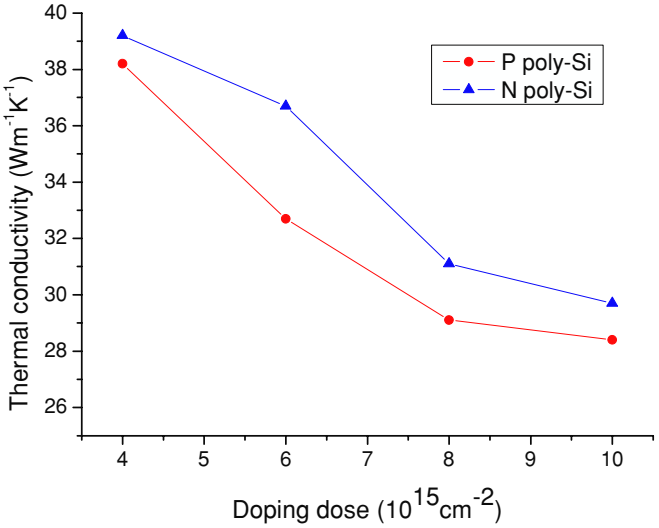

Figure 9. Thermal conductivity of polysilicon at different doping doses.

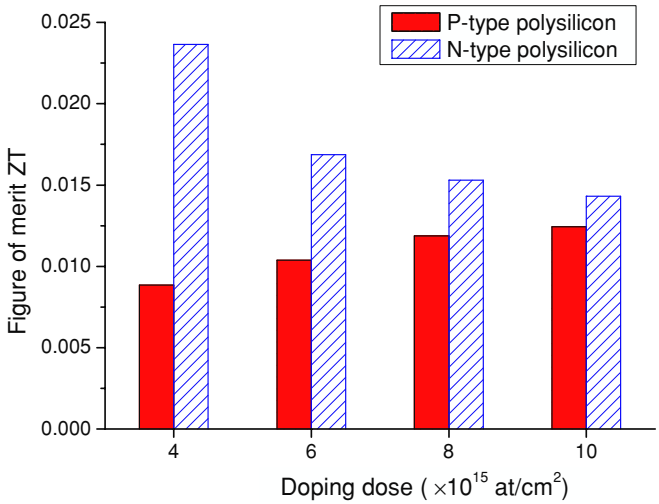

Figure 10. Figure of merit for polysilicon doped with different doses at $T = 300$ K.

p-type polysilicon, the most heavily doped (10×10^{15} at cm^{-2}) has the highest figure of merit, while doping dose of 4×10^{15} at cm^{-2} is the case of highest figure of merit for the n-type polysilicon. This is due to the fact that the Seebeck coefficient of n-type polysilicon with doping dose of 4×10^{15} at cm^{-2} is much higher than the value of the other doping concentrations, while for p-type at this doping concentration the Seebeck coefficient does not increase so much. However, the electrical resistivity at doping dose of 4×10^{15} at cm^{-2} is about twice the value at 10×10^{15} at cm^{-2} for both p-type and n-type polysilicon. When using TPGs to supply power for electronics, the maximum output power is achieved under matched load condition, i.e. the load resistance connected to the generator equals the internal electrical resistance of the generator. Since TPGs based on polysilicon usually have very high internal electrical resistance which is at the level of tens of megaohm [6, 7], it is preferred to make the electrical resistivity of polysilicon as low as possible. As a trade-off between figure of merit and electrical resistivity, the most heavily doped polysilicon, i.e., 10×10^{15} at cm^{-2}, is chosen in fabrication of TPGs. Thermoelectric properties and figure of merit of polysilicon and polySiGe reported in the literature are summarized in table 2. Generally, polySiGe has a much lower thermal conductivity, and thus higher figure of merit, than polysilicon. However, the electrical resistivity of polySiGe is higher than polysilicon, which causes higher internal electrical resistance of power generator based on polySiGe.

Based on the characterization results, a CMOS compatible TPG has been designed and fabricated, as shown in figure 11. The TPG consists of p- and n-doped polysilicon thermopiles, and top and bottom cavities are created to optimize heat flux through the thermal legs. The detailed fabrication steps and materials were presented in [20]. The generator of area 1 cm^2 consists of 125 144 thermocouples and has an internal electrical resistance of $36 \times 10^6\ \Omega$. A graph of the output power per area versus the temperature difference for the fabricated generator is displayed in figure 12. It is found that when 5 K difference is maintained across two sides of the device of size 1 cm^2 and under a matched electrical resistance load, the output power is 1.3 μW, which is 1.3 times higher than the power from the polysilicon TPG reported by Infineon [6]. Recently Yang *et al* have also reported a CMOS based TPG with output power of about 1 μW from 1 cm^2 active area and under 5 K difference [8]. Our approach shows optimized polysilicon TPG performance which is better than reported data from the other groups.

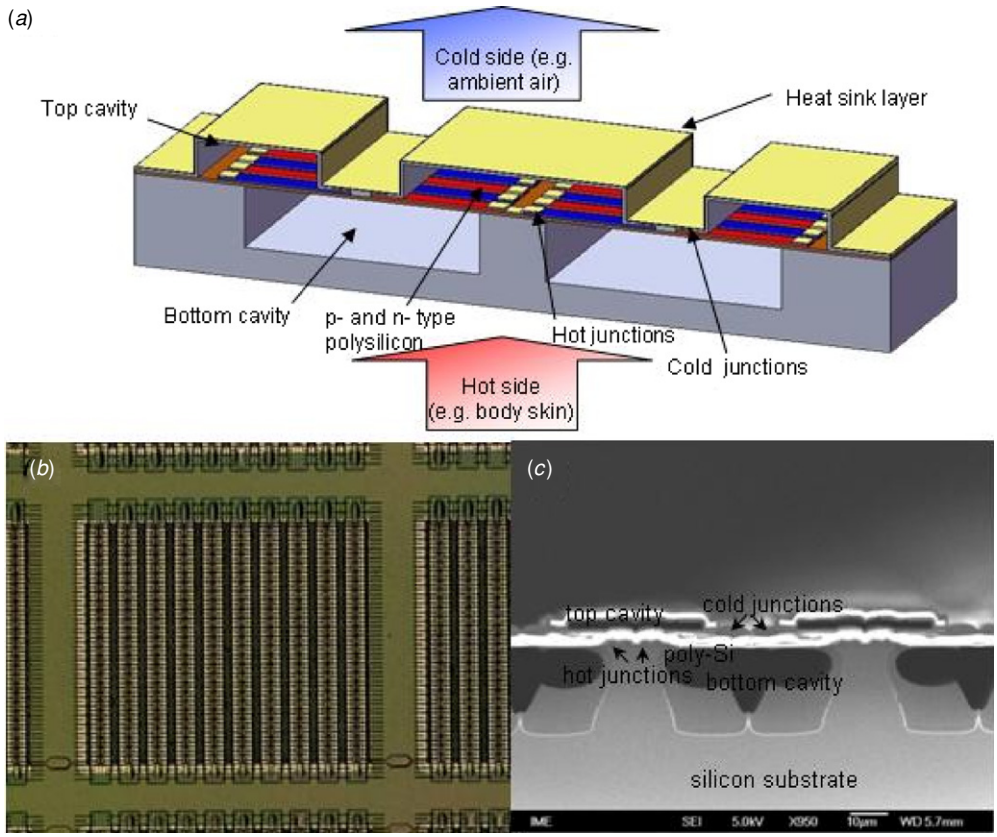

Figure 11. Thermoelectric power generator based on doped polysilicon: (*a*) schematic view, (*b*) top view and (*c*) cross-sectional view.

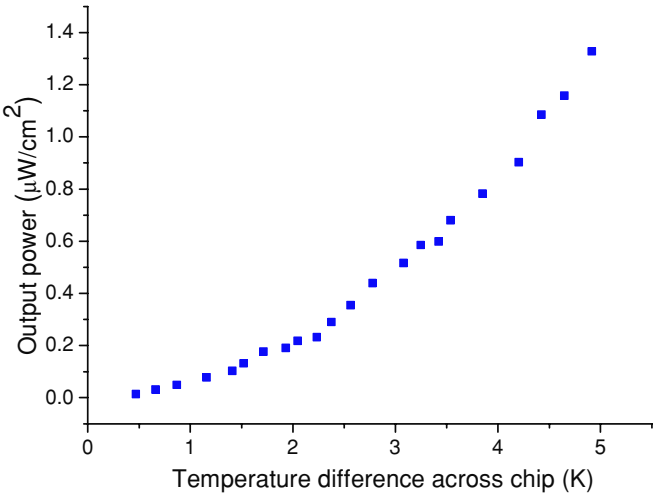

Figure 12. Output power versus temperature difference across the chip.

4. Conclusion

Heavily doped boron and phosphorus LPCVD polysilicon films with different doping doses have been characterized for their thermoelectric performance. Test structures are designed to characterize the electrical resistivity, specific contact resistance, Seebeck coefficient and thermal conductivity at room temperature. The electrical resistivity, Seebeck coefficient and thermal conductivity decrease with increasing doping dose. The formation of nickel silicidiaton between polysilicon and metal greatly reduces the contact resistance. Values of the figure of merit for the polysilicon film doped by different doses are reported. Considering the requirement of low total electrical resistance of the thermoelectric generator, the most heavily doped (10×10^{15} at cm^{-2}) polysilicon film is chosen for the fabrication of the power generator, and the figures of merit for the chosen p- and n-type polysilicon are measured as 0.012 and 0.014, respectively. These results provide good data reference to fabricate thermoelectric power generator of optimal design with high output power.

Acknowledgment

The authors and C Lee, PI of A*STAR HOME 2015 National Research Programme (SERC grant no. 0621150043), would like to thank A*STAR HOME 2015 National Research Programme for the funding of this project and in-kind contribution from Institute of Microelectronics, A*STAR.

References

[1] Leonov V, Torfs T, Fiorini P and Hoof C V 2007 Thermoelectric converters of human warmth for self-powered wireless sensor nodes *IEEE Sensors J.* **7** 650–7

[2] Torfs T, Leonov V and Vullers R J M 2007 Pulse oximeter fully powered by human body heat *Sensors Transducers J.* **80** 1230–38

[3] Bottner H, Nurnus J, Gavrikov A, Kuhner G, Jagle M, Kunzel C, Eberhard D, Plescher G, Schuber A and Schlerth K H 2004 New thermoelectric components using microsysterm technologies *J. Microelectromech. Syst.* **13** 414–20

[4] Hochbaum A I, Chen R, Delgado R D, Liang W, Garnett E C, Najarian M, Majumdar A and Yang P 2008 Enhanced thermoelectric performance of rough silicon nanowires *Nature* **451** 163–7

[5] Boukai A I, Bunimovich Y, Jamil T-K, Yu J-K, Goddard W A and Heath J R 2008 Silicon nanowires as efficient thermoelectric materials *Nature* **451** 168–71

[6] Strasser M, Aigner R, Lauterbach C, Sturm T F, Franosch M and Wachutka G 2004 Micromachined CMOS thermoelectric generators as on-chip power supply *Sensors Actuators* A **114** 362–70

[7] Huesgen T, Woias P and Kockmann N 2008 Design and fabrication of MEMS thermoelectric generators with high temperature efficiency *Sensors Actuators* A **145–146** 423–9

[8] Yang S M, Lee T and Jeng C A 2009 Development of a thermoelectric energy harvester with thermal isolation cavity by standard CMOS process *Sensors Actuators* A **153** 244–50

[9] Graf A, Arndt M, Sauer M and Gerlach G 2007 Review of micromachined thermopiles for infrared detection *Meas. Sci. Technol.* **18** R59–75

[10] Paul O, von Arx M and Baltes H 1995 Process-dependent thermophysical properties of CMOS IC thin films *Proc. Transducers (Stockholm, Sweden, 25–29 Jun. 1995)* pp 178–81

[11] von Arx M, Paul O and Baltes H 1997 Test structures to measure the Seebeck coefficient of CMOS IC polysilicon *IEEE Trans. Semicond. Manuf.* **10** 201–8

[12] von Arx M, Paul O and Baltes H 2000 Process-dependent thin-film thermal conductivities for thermal CMOS MEMS *J. Microelectromech. Syst.* **9** 136–45

[13] Boutchich M, Ziouche K, Godts P and Leclercq D 2002 Characterization of phosphorus and boron heavily doped LPCVD polysilicon films in the temperature range 293–373 K *IEEE Electron Device Lett.* **23** 139–41

[14] McConnell A D, Uma S and Goodson K E 2001 Thermal conductivity of doped polysilicon layers *J. Microelectromech. Syst.* **10** 360–9

[15] Wijngaards D D L and Wolffenbuttel R F 2002 Thermo-electric characterization of APCVD poly$Si_{0.7}Ge_{0.3}$ for IC-compatible fabrication of integrated lateral Peltier elements *IEEE Electron Device Lett.* **23** 139–41

[16] Wang Z, Fiorini P, Leonov V and Hoof C V 2009 Characterization and optimization of polycrystalline $Si_{70\%}Ge_{30\%}$ for surface micromachined thermopiles in human body applications *J. Micromech. Microeng.* **19** 094011

[17] Proctor S J, Linholm L W and Mazer J A 1983 Direct measurement of interfacial contact resistance, end contact resistance, and interfacial contact layer uniformity *IEEE Trans. Electron Devices* **30** 1535–42

[18] Colgan E G, Gambino J P and Hong Q Z 1996 Formation and stability of silicides on polycrystalline silicon *Mater. Sci. Eng.* **R16** 43–96

[19] Deng F, Johnson R A, Asbeck P M and Lau S S 1997 Silicidation process using NiSi and its device application *J. Appl. Phys.* **81** 8047–51

[20] Xie J, Lee C and Feng H 2009 Design, fabrication and characterization of CMOS MEMS based thermoelectric power generators *J. Microelectromech. Syst.* at press